J Solid State Electrochem (2015) 19:1247–1252
DOI 10.1007/s10008-015-2746-6

SHORT COMMUNICATION

Morphological changes in electrochemically deposited poly(3,4-ethylenedioxythiophene) films during overoxidation

M. Ujvári · J. Gubicza · V. Kondratiev · K. J. Szekeres · G. G. Láng

Received: 25 November 2014 / Revised: 4 January 2015 / Accepted: 6 January 2015 / Published online: 14 January 2015

Abstract Electrochemical and morphological properties of thin poly(3,4-ethylenedioxy-thiophene) (PEDOT) films deposited on gold were investigated in aqueous sulfuric acid solutions. X-ray diffraction and electron microscopy were used for monitoring the morphological changes and structure evolution caused by overoxidation. The diffraction peaks of PEDOT became sharper and more intensive during the subsequent oxidation cycles. This indicates that besides the degradation of the PEDOT film, its crystallinity was gradually improved with increasing the number of oxidation cycles. These changes may result in the appearance of novel properties that may be advantageous for specific applications.

Keywords Overoxidation of PEDOT · Crystalline phase · Scanning electron microscopy · X-ray diffraction · Sensors

Introduction

Conductive polymers are used in a variety of applications that require materials which are both electrically conducting and mechanically compliant. Electronic and electrochemical devices based on organic materials are, e.g., light-emitting diodes, organic thin-film transistors, solar cells, memory devices, ion-selective electrodes, microelectrode arrays, fuel cells, etc. [1–15]. Beyond doubt, the monitoring of the degradation of the polymer layers is of great importance for the long-term use of these devices.

Among the organic conducting polymers, poly(3,4-ethylenedioxythiophene) [16], often abbreviated as PEDOT, and its derivatives appear to be among the most stable organic conducting polymers currently available. Previous studies have shown that PEDOT is highly insoluble in almost every solvents, is electroactive in aqueous solutions [17–19], and exhibits a relatively high conductivity. On the basis of these results, studies have been performed to investigate the electrochemistry of PEDOT in more detail, e.g., by using cyclic voltammetry (CV). It has been found in refs. [20–22] that when the positive potential limit of the CV is extended into the region in which the overoxidation of the polymer film takes place, an oxidation peak (without a corresponding reduction peak) appears, but only minor changes can be observed in the properties of the cyclic voltammograms recorded in the "stability region" before and after overoxidation.

In refs. [16] and [22], it has been shown that PEDOT films deposited on Au or Pt undergo structural changes during the overoxidation (degradation) process. The most probable stages involved in the overoxidation/delamination process are as follows: (i) overoxidation results in stress generation in the PEDOT film [23]; (ii) formation of cracks due to internal stress; (iii) the residual products of the degradation of the polymer leave the polymer layer; (iv) after the formation of the line cracks, the film stress is partially released; (v) the partial delamination of the polymer layer leads to exposure of the underlying metal substrate to the electrolyte solution; (vi) The polymer film still present on the substrate after overoxidation remains electroactive; and (vii) The areas with the polymer form a barrier between the metal substrate and the surrounding electrolyte solution.

M. Ujvári · K. J. Szekeres · G. G. Láng (✉)
Institute of Chemistry, Department of Physical Chemistry, Laboratory of Electrochemistry and Electroanalytical Chemistry, Eötvös Loránd University, Pázmány P. s. 1/A, H-1117, Budapest, Hungary
e-mail: langgyg@chem.elte.hu

J. Gubicza
Institute of Physics, Department of Materials Physics, Eötvös Loránd University, Pázmány P. s. 1/A H-1117, Budapest, Hungary

V. Kondratiev
Chemical Department, St. Petersburg State University, Universitetskii pr. 26, St. Petersburg 198504, Russia

Although the above conclusions seem to be justified, the internal structure of the polymer film remaining on the substrate after the overoxidation process has not been investigated in the papers mentioned above. This topic may, however, be an interesting subject for further studies, since according to literature, reports conducting polymers in different overoxidation states show unique features useful for analytical, sensing, and biomedical applications [24–27].

For instance, many studies have demonstrated that overoxidized polypyrrole films exhibit molecular-sieve properties and such films have been used to fabricate glucose, alcohol, hydrazine, and dopamine sensors [25–32]. A demonstration of an organic electronic ion pump containing parts made of overoxidized PEDOT:PSS (poly(3,4-ethylenedioxythiophene):poly(styrenesulfonate)) was provided in refs. [27, 33]. In [34], oxidized PEDOT films were successfully used for sensing perchlorate. It is also well known that in conductive polymer-based ion, bipolar junction transistors emitter and collector are cation selective and contain overoxidized PEDOT [35, 36]. According to [37], an overoxidized poly(3,4-ethylenedioxythiophene) film-modified screen-printed carbon electrode exhibited superior sensitivity and selectivity for the recognition of electrochemical probes, leading to the determination of submicromolar concentration of dopamine without interference from the existing ten times of concentration of uric acid and 1000 times of concentration of ascorbic acid. The basis for the observed selectivity of overoxidized polymer films is not entirely clear. In some cases, it is attributed to the increase in porosity of the polymer film [32, 38].

The purpose of the present paper is to complement (and extend) the results reported in [21] and [22] by studying the morphological changes in electrodeposited PEDOT films during overoxidation. As it has been pointed out in [22], the overoxidation/degradation of PEDOT films can result in random-like, but quite well-ordered arrays of islands and trench-like structures. This may imply an increase of the crystalline fraction in the polymer layer. In the present work, we tried to check this assumption. In order to gain a deeper insight into these issues, X-ray diffraction along with electron microscopy was used for monitoring the structure evolution of the films during the overoxidation process.

Experimental

Solutions and film preparation

The gold/poly(3,4-ethylenedioxythiophene) films were prepared by electro-polymerization from 0.01 mol dm^{-3} ethylenedioxythiophene (EDOT)/0.1 mol dm^{-3} Na_2SO_4 solution under galvanostatic conditions. The PEDOT films were formed on gold plates or on gold layers deposited by vacuum evaporation onto glass substrates. A constant current density of 0.2 mA cm^{-2} was applied for 7200 s. Analytical grade 3,4-ethylenedioxythiophene (Aldrich), p.a. Na_2SO_4 (Fluka), and ultra-pure water (specific resistance 18.3 MΩ cm) were used for solution preparation. The 0.1 M H_2SO_4 solutions used for voltammetric experiments were prepared with ultra-pure water and p.a. H_2SO_4 (Merck). All solutions were purged with

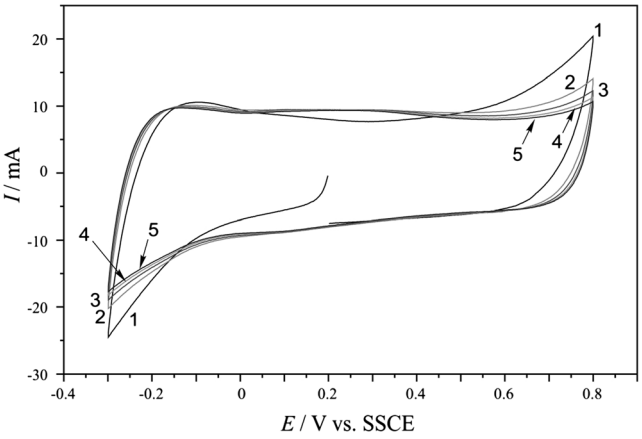

Fig. 1 The cyclic voltammograms recorded in 0.1 M aqueous solution of H_2SO_4 (scan rate ν=50 mV s^{-1}). The curves have been selected from a series of 40 repeated scans recorded immediately after the preparation of the PEDOT film. *1*: 1st scan; *2*: 10th scan; *3*: 20th scan; *4*: 30th scan; *5*: 40th scan

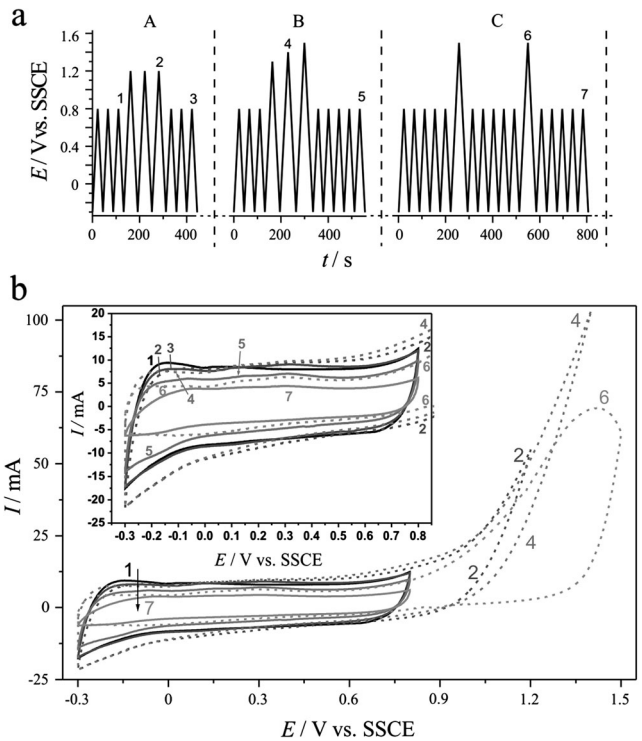

Fig. 2 **a** Potential program applied to the Au | PEDOT | 0.1 M sulphuric acid electrode. Sweep rates ν=50 mV s^{-1}. *A*, *B*, and *C* are time intervals, after which XRD patterns presented in Fig. 6 were recorded. **b** Cyclic voltammograms corresponding to the cycles marked with *1–7* in **a**

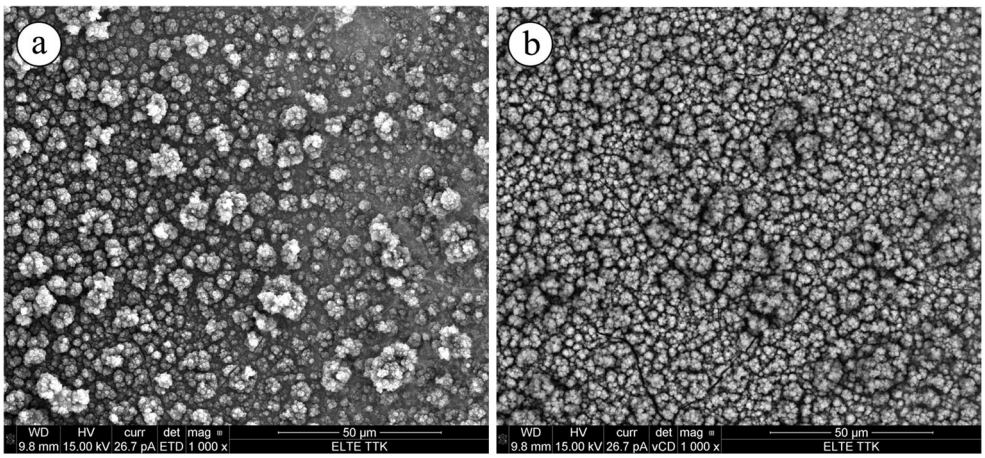

Fig. 3 SEM images of the freshly prepared PEDOT film. **a** SEM image using secondary electrons. **b** the corresponding backscattered SEM image taken from the same area. The length of the *horizontal white bar* below the images corresponds to 50 μm

oxygen-free argon (Linde 5.0) before use, and an inert gas blanket was maintained throughout the experiments.

An Autolab PGSTAT 20 potentiostat was used to control the electrochemical cell operations and data acquisition. The film thickness ($d \approx 2.9$ μm) was estimated from the amount of charge passed in the deposition of the PEDOT film and by using the charge/film volume ratio determined earlier by direct thickness measurements [39, 40]. The thickness of the films investigated in the present work was about two times larger than that reported in [21] and [22] since thicker films were required to obtain reliable X-ray diffraction data.

Voltammetry

The conventional three-electrode cell configuration was used. A high surface area gold-foil was arranged cylindrically around the working electrode to maintain a uniform electric field (counter electrode). A NaCl-saturated calomel electrode (SSCE) was used as the reference.

Scanning electron microscopy

The oxidation of the polymer film has been followed with scanning electron microscopy. A Quanta™ 3D FEG high-resolution, low-vacuum scanning electron microscopy (SEM)/FIB instrument was used for SEM analysis.

X-ray diffraction

The phase composition of PEDOT was studied by X-ray diffraction using a Philips Xpert powder diffractometer with CuKα radiation (wavelength 0.15418 nm) and Bragg-Brentano geometry [41].

Results and discussion

Cyclic voltammetry

In the potential interval −0.3–0.8 V vs. SSCE the PEDOT films are remarkably stable, retaining their properties even

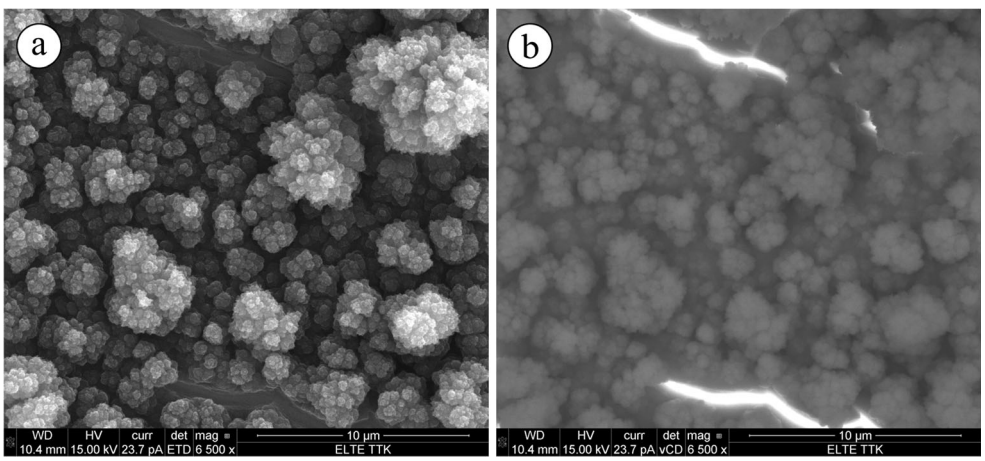

Fig. 4 SEM images of the PEDOT film prepared on gold after the application of 40 potential cycles (ν=50 mV s^{-1}) in the range from −0.3 to 0.8 V vs. SSCE (see Fig. 1). **a** SEM image using secondary electrons. **b** the corresponding backscattered SEM images taken from the same area. The length of the *horizontal white bar* below the images corresponds to 10 μm

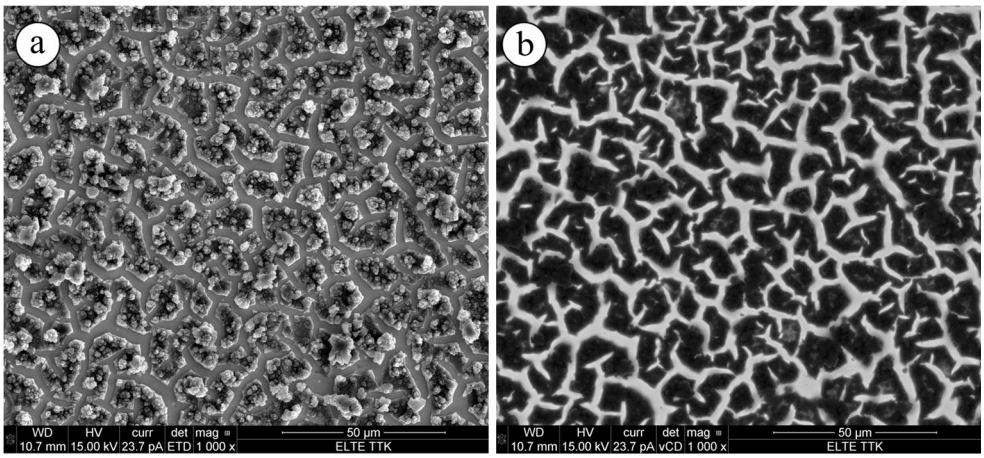

Fig. 5 SEM images of the PEDOT film recorded after time interval *C* in Fig. 2a (overoxidized film). **a** SEM image using secondary electrons. **b** The corresponding backscattered SEM images taken from the same area. The length of the *horizontal white bar* below the images corresponds to 50 μm

after several consecutive cyclic voltammetric scans. The cyclic voltammograms in Fig. 1 have been selected from a series of 40 scans which were recorded in 0.1 M aqueous sulfuric acid solution (scan rate ν=50 mV s^{-1}) immediately after the first X-ray diffraction (XRD) measurement performed on the freshly made film (see curve 1 in Fig. 6, geometric surface area of the film 4.0 cm^2). As it can be seen from the figure, the oxidation-reduction process is reversible, if the positive electrode potential limit is kept below 0.8 V vs. SSCE. Except for the first scan, the capacitances at the corresponding electrode potentials remained almost unchanged with the increasing number of potential cycles. A similar conclusion is true for the X-ray powder diffractograms taken before and after the potential cycling treatment: patterns characteristic for an amorphous state have been identified in the sample in both cases (see Fig. 6, curves 1 and 2).

Cyclic voltammetric curves recorded for the gold | PEDOT | 0.1 M sulfuric acid (aq) electrode (geometric surface area 4.0 cm^2) at a sweep rate of ν=50 mV s^{-1} are presented in Fig. 2b. The potential program applied to the electrode is given in Fig. 2a. Three time intervals in Fig. 2a are marked by "A," "B," and "C". According to the results, irreversible oxidation of the PEDOT film starts at or above 0.8 V vs. SSCE. The shapes of the cyclic voltammograms change considerably if the electrode potential exceeds this value ("overoxidation cycles": see, e.g., curves 2, 4, and 6 in Fig. 2b), an oxidation peak with no corresponding reduction peak can be observed at potentials above 0.8 V. By comparing, e.g., curve 1 and curve 3 in Fig. 2b, it can be seen that there are only small differences between the voltammograms recorded in the −0.3–0.8-V potential range before and after three overoxidation cycles taken between −0.3 and 1.2 V. However, if the positive limit of the electrode potential is extended to 1.5 V vs. SSCE, the intensity of the redox response (i.e., the capacitance of the film) gradually decreased (see curves 3, 5, and 7 in Fig. 2b). Nevertheless, curve 7 still shows the presence of a significant amount of polymer in direct (electrical) contact with the gold surface.

SEM micrographs of the PEDOT layers on Au

The SEM images of the PEDOT film prepared freshly on gold are presented in Fig. 3a. One can see in the image detected by secondary electrons (SE) that well-separated globules (or cauliflower-like particles) are present on the top of the polymer layer. The backscattered electron (BSE) micrograph taken from the same area (which characterizes a thicker layer compared to SE) shows that the globules are attached to an underlying smoother polymer layer (Fig. 3b).

Figure 4a, b shows SEM images of the PEDOT film prepared on gold after the application of 40 potential cycles (CV-s) at 50 mVs^{-1} in the range from −0.3 to 0.8 V vs. SCE. The most striking difference between the micrograph shown in Fig. 4a and that of the freshly prepared sample in Fig. 3a is the appearance of some narrow cracks or crevices in the SEM image of the oxidized film. The cracks results in bright spots ("islands") in the backscattered SEM images (Fig. 4b). The formation of the cracks can be well explained as the result of internal stress changes in the thick polymer film [21–23].

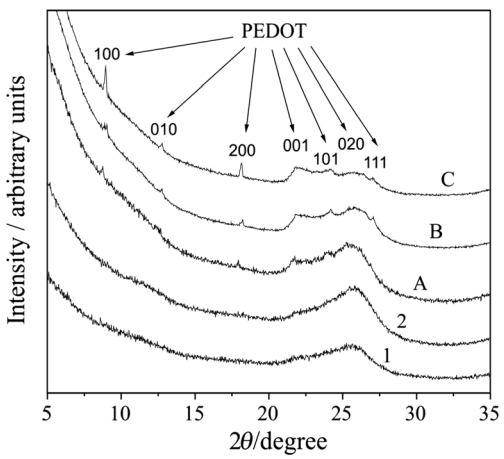

Fig. 6 X-ray diffractograms. *1*: freshly prepared PEDOT film; *2*: PEDOT film after the application of 40 potential cycles (ν=50 mV s^{-1}) in the range from −0.3 to 0.8 V vs. SSCE (see Fig. 1); *A*, *B*, *C*: obtained after time intervals A, B, and C in Fig. 2a, respectively

Figure 5a, b shows SE and BSE SEM images, respectively, for the PEDOT film after the time interval C in Fig. 2a. The most striking difference between the micrograph shown in Fig. 5a and that of the freshly prepared sample in Fig. 3a is the appearance of a network of grooves (narrow trench-like structures). The width of the crevices shown in Fig. 5a is about 2–3 μm. According to the backscattered SEM micrographs (Fig. 5b), the crevices are interconnected and form a widespread network. EDX analysis proved that only Au is present at the bottom of the grooves.

X-ray diffraction

The powder diffractograms obtained for the initial state (curve 1), after 40 consecutive cyclic voltammetric scans in the potential interval −0.3–0.8 V vs. SSCE (curve 2), and after the time intervals A, B, and C specified in Fig. 2a are shown in Fig. 6 (curves A, B, and C). Partial crystallinity with well-separated X-ray diffraction peaks is observed in the overoxidized PEDOT film (curves A, B, and C) while a pattern characteristic for an amorphous state is identified in the samples without overoxidation (curves 1 and 2). This proves directly that the crystallization is the result of overoxidation and not of the potential cycling alone.

The diffraction peaks of crystalline PEDOT were indexed according to previous studies [42, 43]. These works identified this phase as orthorhombic structure. The best agreement between the theoretical orthorhombic and the experimental peak positions was obtained by selecting the following values for the three lattice parameters: a=0.980, b=0.690, and c=0.405 nm. The value of b is very close to the lattice constant (b=0.679 nm) determined from reflection 020 in a previous study [43]. However, it should be noted that the values of the lattice parameters of PEDOT are very sensitive on the type of counter ion as revealed in Table 2.1 of ref. [43]. Figure 6 shows that the diffraction peaks of PEDOT became sharper and more intensive due to electrochemical treatment (curves A, B, and C). This indicates that besides the degradation of the PEDOT film, its crystallinity was gradually improved with increasing the number of oxidation cycles.

Conclusions

According to the above experimental results, the originally compact and strongly adherent PEDOT films undergo structural changes during over oxidation. The porosity of the film increases progressively during the degradation process. X-ray diffraction results showed that besides degradation, the crystallinity of the PEDOT film was also gradually improved with increasing number of overoxidation cycles. These changes may result in the generation of sites with novel catalytic and binding properties that may be advantageous for specific applications.

Acknowledgments Financial support from the Hungarian Scientific Research Fund (grant nos. K 109021 and K 109036) and from the Russian Foundation for Basic Research (grant N-13-03-00984) is gratefully acknowledged. The authors thank Prof. K. Havancsák and Prof. G. Varga for the SEM measurements and for helpful discussions. The project was supported by the European Union and co-financed by the European Social Fund (grant agreement no. TAMOP 4.2.1/B-09/1/KMR-2010-0003).

References

1. Kvarnström C (2012) Conducting polymers. In: Bard AJ, Inzelt G, Scholz F (eds) Electrochemical dictionary, 2nd edn. Springer, Heidelberg
2. Inzelt G (2012) Conducting polymers. A new era in electrochemistry. In: Scholz F (ed) Monographs in electrochemistry, 2nd edn. Springer, Berlin Heidelberg
3. Lang U, Naujoks N, Dual J (2009) Synth Met 159:473–479
4. Inzelt G (1994) In: Bard AJ (ed) Electroanalytical chemistry, vol 18. New York, Marcel Dekker
5. Wang GF, Tao XM, Wang RX (2008) Nanotechnology 19:145201–145202
6. Inzelt G, Pineri A, Schultze JW, Vorotyntsev MA (2000) Electrochim Acta 45:2403–2421
7. Lilliedal MR, Medford AJ, Madsen MV, Norrman K, Krebs FC (2010) Sol Energy Mater Sol Cells 94:2018–2031
8. Nasybulin E, Wei S, Cox M, Kymissis I, Levon K (2011) J Phys Chem C 115:4307–4314
9. Scott JC (2004) Science 304:62–63
10. Möller S, Perlov C, Jackson W, Taussig C, Forrest SR (2003) Nature 426:166–169
11. Cui X, Martin DC (2003) Sensors Actuators B Chem 89:92–102
12. Vázquez M, Danielsson P, Bobacka J, Lewenstam A, Ivaska A (2004) Sensors Actuators B Chem 97:182–189
13. Bobacka J (1999) Anal Chem 71:4932–4937
14. Drillet JF, Dittmeyer R, Jüttner K, Li L, Mangold KM (2006) Fuel Cells 6:432–438
15. Drillet JF, Dittmeyer R, Jüttner K (2007) J Appl Electrochem 37:1219–1226
16. Kvarnström C (2012) Poly(thiophene). In: Bard AJ, Inzelt G, Scholz F (eds) Electrochemical dictionary, 2nd edn. Springer, Heidelberg
17. Bobacka J, Lewenstam A, Ivaska A (2000) J Electroanal Chem 489:17–27
18. Yamato H, Ohwa M, Wernet W (1995) J Electroanal Chem 397:163–170
19. Sakmeche N, Aeiyach S, Aaron JJ, Jouini M, Lacroix JC, Lacaze PC (1999) Langmuir 15:2566–2574
20. Zykwinska A, Domagala W, Pilawa B, Lapkowski M (2005) Electrochim Acta 50:1625–1633
21. Ujvári M, Takács M, Vesztergom S, Bazsó F, Ujhelyi F, Láng GG (2011) J Solid State Electrochem 15:2341–2349
22. Láng GG, Ujvári M, Bazsó F, Vesztergom S, Ujhelyi F (2012) Electrochim Acta 73:59–69
23. Láng GG, Barbero C (2012) Laser techniques for the study of electrode processes. In: Scholz F (ed) Monographs in electrochemistry. Springer, Berlin
24. Li J, Lin X-Q (2007) Sens Actuators B 124:486–493
25. Martin DC, Wu J, Shaw CM, King Z, Spanninga SA, Richardson-Burns S, Hendricks J, Yang J (2010) Polym Rev 50:340–384

26. Zhuang Z, Li J, Xu R, Xiao D (2011) Int J Electrochem Sci 6:2149–2161
27. Irimia-Vladu M (2014) Chem Soc Rev 43:588–610
28. Majidi MR, Jouyban A, Asadpour-Zeynali K (2007) Electrochim Acta 52:6248–6253
29. Tu X, Xie Q, Jiang S, Yao S (2007) Biosens Bioelectron 22:2819–2826
30. Wen J, Zhou L, Jin L, Cao X, Ye B-C (2009) J Chromatogr B 877: 1793–1798
31. Li Y, Wang P, Wang L, Lin X (2007) Biosens Bioelectron 22:3120–3125
32. Boateng A, Iraque F, Brajter-Toth A (2013) Electroanalysis 25:345–355
33. Simon DT, Kurup S, Larsson KC, Hori R, Tybrandt K, Goiny M, Jager EWH, Berggren M, Canlon B, Richter-Dahlfors A (2009) Nat Mater 8:742–746
34. Bendikov TA, Harmon TC (2005) Anal Chim Acta 551:30–36
35. Ranjan N, Reddy AHM (2014) Appl Mech Mater 490(491):123–128
36. Tybrandt K, Larsson KC, Richter-Dahlfors A, Berggren M (2010) Proc Natl Acad Sci U S A 107:9929–9932
37. Lin J-M, Su Y-L, Chang W-T, Su W-Y, Cheng S-H (2014) Electrochim Acta 149:65–75
38. Boateng A, Cohen-Shohet R, Brajter-Toth A (2011) Electrochim Acta 56:7651–7658
39. Stoyanova A, Tsakova V (2010) J Solid State Electrochem 14:1947–1955
40. Poppendieck W, Hoffmann KP (2009) In: Vander Sloten J, Verdonck P, Nyssen M, Haueisen J (eds) ECIFMBE 2008, IFCMBE proceedings 22. Springer-Verlag Berlin, Heidelberg, pp 2409–2412
41. Klug HP, Alexander LE (1974) X-ray diffraction procedures for polycrystalline and amorphous materials. Wiley, New York
42. Wu J (2011) Morphology of poly(3,4-ethylene dioxythiophene) (PEDOT) thin films, crystals, cubic phases, fibers and tubes, PhD dissertation, The University of Michigan
43. Takano T, Masunaga H, Fujiwara A, Okuzaki H, Sasaki T (2012) Macromolecules 45:3859–3865